Biophysical characterization and stability of modified IgG1 antibodies with different hexamerization propensities

Kampen, M.D. van; Kuipers-De Wilt, L.H.A.M.; Egmond, M.L. van; Reinders-Blankert, P.; Bremer, E.T.J. van den; Wang, G.B.; ... ; Jong, R.N. de

Journal of Pharmaceutical Sciences 111 (2022) 1587–1598

Contents lists available at ScienceDirect

Journal of Pharmaceutical Sciences

journal homepage: www.jpharmsci.org

Pharmaceutical Biotechnology

Biophysical Characterization and Stability of Modified IgG1 Antibodies with Different Hexamerization Propensities

Muriel D. van Kampen[a], Leonie H.A.M. Kuipers-De Wilt[a], Mariëlle L. van Egmond[a], Petra Reinders-Blankert[a], Ewald T.J. van den Bremer[a], Guanbo Wang[b,c,1], Albert J.R. Heck[b,c], Paul W.H.I. Parren[d,2], Frank J. Beurskens[a], Janine Schuurman[a], Rob N. de Jong[a,*]

[a] Genmab, Uppsalalaan 15, 3584 CT Utrecht, the Netherlands
[b] Biomolecular Mass Spectrometry and Proteomics, Bijvoet Center for Biomolecular Research and Utrecht Institute for Pharmaceutical Sciences, Utrecht University, 3584 CH Utrecht, the Netherlands
[c] Netherlands Proteomics Centre, 3584 CH Utrecht, the Netherlands
[d] Department of Immunohematology and Blood Transfusion, Leiden University Medical Center, Leiden, the Netherlands

ARTICLE INFO

Article history:
Received 3 September 2021
Revised 24 February 2022
Accepted 24 February 2022
Available online 27 February 2022

Keywords:
Reversible self-association
Hexamerization
Developability
Biophysical properties
Conformational and Colloidal stability
HexaBody

ABSTRACT

The hexamerization of natural, human IgG antibodies after cell surface antigen binding can induce activation of the classical complement pathway. Mutations stimulating Fc domain-mediated hexamerization can potentiate complement activation and induce the clustering of cell surface receptors, a finding that was applied to different clinically investigated antibody therapeutics. Here, we biophysically characterized how increased self-association of IgG1 antibody variants with different hexamerization propensity may impact their developability, rather than functional properties. Self-Interaction Chromatography, Dynamic Light Scattering and PEG-induced precipitation showed that IgG variant self-association at neutral pH increased in the order wild type (WT) < E430G < E345K < E345R < E430G-E345R-S440Y, consistent with functional activity. Self-association was strongly pH-dependent, and single point mutants were fully monomeric at pH 5. Differential Scanning Calorimetry and Fluorimetry showed that mutation E430G decreased conformational stability. Interestingly, heat-induced unfolding facilitated by mutation E430G was reversible at 60°C, while a solvent-exposed hydrophobic mutation caused irreversible aggregation. Remarkably, neither increased dynamic self-association propensity at neutral pH nor decreased conformational stability substantially affected the stability of concentrated variants E430G or E345K during storage for two years at 2-8°C. We discuss how these findings may inform the design and development of IgG-based therapeutics.

Introduction

Therapeutic monoclonal antibodies are widely used to treat a range of diseases including cancer and inflammatory diseases. Despite the clinical and commercial success of current antibody therapeutics, there is broad interest in developing next generation antibody designs with improved properties. Antibody formats have been engineered to modulate specificity, stability, in vivo pharmacokinetics, and Fc effector functions of therapeutic antibodies.[1-3] The activation of Fc-effector functions can also be strongly promoted by the formation of antibody clusters or aggregates.[4-6]

During natural immune reactions against pathogens and self-antigens, the association of natural IgG antibodies into complexes at self- or pathogenic surfaces may lead to the activation of the complement system, an innate immune defense mechanism.[7] After antigen binding,

Abbreviations: B_{22}, Osmotic second virial coefficient; CDC, Complement-Dependent Cytotoxicity; CE-SDS, Capillary Electrophoresis – Sodium Dodecyl Sulfate; C_H2-C_H3, constant domains of the heavy chain; DLS, Dynamic Light Scattering; DSC, Differential Scanning Calorimetry; DSF, Differential Scanning Fluorimetry; HP-SEC, High Performance Size-Exclusion Chromatography; MS, Mass Spectrometry; PEG, Poly-Ethylene Glycol; SIC, Self-Interaction Chromatography; T_{agg}, Onset of aggregation temperature; T_m, melting temperature; WT, Wild Type.

This article contains supplementary material available from the authors by request or via the Internet.

* Correspondence to.
E-mail address: rjo@genmab.com (R.N. de Jong).
[1] Current address: Biomedical Pioneering Innovation Center, Peking University, 5 Yiheyuan Rd, Haidian District, Beijing 100871, P.R. China
[2] Current address: Lava Therapeutics, Utrecht, the Netherlands.

https://doi.org/10.1016/j.xphs.2022.02.016

initiation of the classical complement pathway can be triggered by the formation of ordered, ring-like structures of six antibodies (hexamers) on the cell surface with a diameter of approximately 25 nm. These hexamers bind and activate C1, the first component of the complement system, which may lead to target cell killing via Complement Dependent Cytotoxicity (CDC).[8] We observed that IgG molecules containing a single mutation such as E430G or E345K, located in the antibody C_H3 domain, promote interactions between Fc-domains after cell surface binding, leading to enhanced hexamer formation.[9] This process of controlled, antigen binding-dependent hexamerization can be applied to promote CDC induction, or to promote outside-in signaling by cell surface receptors.[10, 11] Multiple products based on this antibody technology platform, termed HexaBody, have entered clinical investigation.

In addition to the natural process of IgG hexamerization after antigen binding, therapeutic antibodies can form aggregates via other pathways, comprehensively reviewed by Roberts.[12] Small oligomeric clusters (molecular aggregates) can be formed upon self-association of folded or partially unfolded monomers and initially these aggregates are often present in a reversible state (referred to as reversible self-association). However, small clusters can grow into irreversible aggregates eventually leading to macro particle formation and phase separation.[12, 13] In particular non-native, irreversible aggregation may compromise protein quality, and the process of aggregation can considerably impact shelf life.[14] Antibody aggregates and aggregation mechanisms have been extensively characterized also because of their potential impact on increased immunogenicity and loss of efficacy.[15, 16] In addition, adverse effects can be caused by the formation of immune complexes composed of drugs and anti-drug antibodies.[17]

Reversible self-association of antibodies can be influenced by molecular and structural properties including surface hydrophobicity, net charge, charge distribution and charge heterogeneity.[18, 19] Combined electrostatic and hydrophobic/aromatic interactions have been proposed as mechanism of reversible self-association.[18] Both Fab-Fab interactions and Fc-domain mediated interactions can contribute to self-association/aggregation of antibodies.[18, 20-23] Protein concentration plays a major role in the self-association process, attributed to the existence of equilibrium conditions, and the high concentrations frequently applied in formulated antibody drug products may induce (reversible) self-association. Upon dilution, as usually performed for analytical assays, reversible aggregates can dissociate into monomers due to the dynamic nature of the monomer-oligomer equilibrium. The strength of protein-protein interactions and self-association propensity can be modulated by formulation conditions, like pH, ionic strength and the presence of excipients.

Previously published characterizations of antibodies with engineered hexamerization propensity focused heavily on their functional properties at concentrations relevant to *in vivo* applications.[9, 24] Here, we perform focused biophysical characterization of model antibody variants with engineered hexamerization propensity at elevated concentrations relevant to pharmaceutical development, to improve our understanding of the impact of antibody self-association on their biophysical behavior and long-term stability in different formulations. We examined the influence of reversible self-association promoted by Fc-Fc interactions on the colloidal stability and long-term stability of HexaBody-derived model compounds with stepwise increasing hexamerization propensity. We also investigated the conformational stability of these molecules.

Results

IgG Hexamerization is a Dynamic Equilibrium Sensitive to IgG Concentration and pH

Multiple HexaBody-derived model compounds with different hexamerization propensities were selected for this study: IgG1 wild type (WT), single mutants E430G, E345K, E345R and triple mutant E345R/E430G/S440Y (RGY). Self-association leads to the formation of a donut-like hexameric structure, with the heavy chain C-termini collected in the central cavity (Fig. 1A). Mutation E345K is located at the intermolecular Fc-Fc interface, while E430G was designed to enhance Fc-domain flexibility by removing an ionic salt bridge between lysine K338 and glutamic acid E430 at the intramolecular C_H2-C_H3 domain interface. Mutants E430G and E345K, with a single mutation in the IgG1 C_H3 domain, retained their monomeric nature in solution at physiologically relevant concentrations, whereas variant E345R induced low levels of IgG hexamer formation already in solution.[9, 24] Triple mutant RGY formed both monomeric and hexameric species co-existing in solution, as previously demonstrated using native Mass Spectrometry (MS), Cryo-Electron Microscopy, High-Speed Atomic Force Microscopy, and size exclusion chromatography coupled to Multiple Angle Light Scattering (SEC-MALS). [8,24-26] In addition to hexamers and monomers, also oligomers of intermediate sizes were detected at low abundance by all four methods, which may suggest a dynamic interconversion between the different oligomeric states.[9, 24, 26]

The high abundance of hexamer species for IgG1-RGY facilitates biophysical characterization of the IgG hexamerization process. Aiming to expand our previous functional characterization of antibody IgG1-2F8-RGY (anti-EGFR)[24] with different biophysical analyses, we now analyzed the monomer-hexamer equilibrium of the RGY variant in more detail by HP-SEC at different concentrations, using PBS pH 7.4 as mobile phase. As expected for a dynamic equilibrium, the hexamer abundance increased with antibody concentration (Fig. 1B and S1). A method-inherent limitation of the SEC is that the equilibrium might be affected by the dilution upon injection, the time in the auto-sampler after dilution of the samples, and the time on the column (flow rate), implying that actual levels of hexamers could be underestimated. SEC analysis is also limited in the dynamic range of its separating power and large aggregates may be filtered out by the guard column. Dynamic Light Scattering analysis as described further below is more appropriate for evaluation of the potential presence of aggregates larger than hexamer size.

To assess the influence of pH on the hexamerization equilibrium, we analyzed IgG1-2F8-RGY by HP-SEC using mobile phases with pH values ranging from pH 7.0 to pH 5.0 (Fig. 1C). A decrease in pH resulted in a decrease in hexamer abundance and a concomitant increase in monomeric species. At pH 5.0, the hexamer species completely disappeared, indicating that low pH caused dissociation of the hexamers into its monomeric components. To study the reversibility of pH-induced dissociation of IgG hexamers, samples of IgG1-2F8-RGY at pH 7.0 were buffer exchanged to pH 5.0 and back to pH 7.0 again. Analytical samples collected at each step were analyzed by HP-SEC using mobile phases with corresponding pH (Fig. 1D). Lowering the pH from 7.0 to 5.0 resulted in dissociation of the hexameric species, but raising the pH of the same sample back to 7.0 fully recovered hexamer formation. To assess if this pH-dependent association may be antibody-specific or inherent to Fc-Fc interactions, we performed an analysis of a different antibody, the functionally characterized IgG1-005-RGY (anti-CD38)[24], using an alternative method, yet still observed essentially similar behavior. Native mass spectrometry indicated that decreasing the pH induced dissociation of hexamers of IgG1-005-RGY to undetectable levels at pH 5.5 (Fig. 1E, S2), indicating that the Fc mutations are likely responsible for the hexamerization behavior. These results demonstrate that hexameric and monomeric IgG exist in an IgG concentration-dependent equilibrium, and that pH may be used to reversibly dissociate and re-associate hexamers of IgG1-RGY.

The pH dependence of IgG1-RGY hexamer formation suggests the involvement of protonation/deprotonation of charged groups such as histidine residues, which contain mildly basic side chains with a

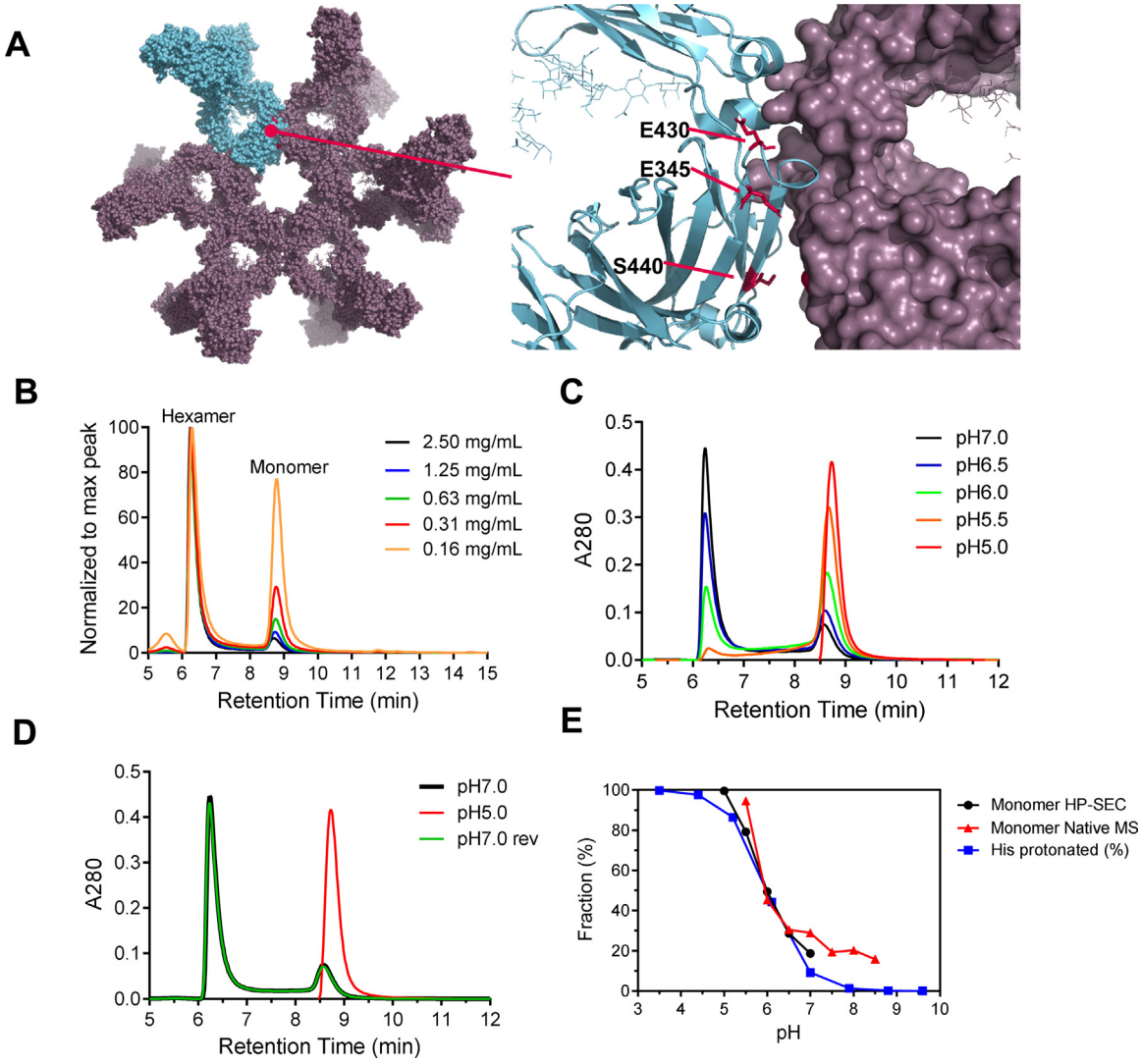

Figure 1. Hexamer structure and Concentration/pH dependence of hexamer formation. (A) Hexamer structure and mutated amino acids. Left panel: Structure of hexameric IgG (PDB access code 1HZH), with one IgG highlighted in blue. Right panel: Structural detail of two adjacent Fc-domains, with the mutated amino acids highlighted in red. Residues E430, E345 and S440 are indicated. (B) Size Exclusion chromatograms of IgG1-2F8-RGY injected at different concentrations in PBS pH 7.4. Peaks are normalized to the intensity of the highest peak. (C) Size Exclusion chromatograms of IgG1-2F8-RGY analyzed with mobile phases of different pH. (D) Reversibility of hexamer formation. The IgG1-2F8-RGY was formulated in pH 7.0 (black), buffer exchanged to pH 5.0 (red) and buffer exchanged back to pH 7.0 (green). (E) Histidine protonation/deprotonation as mechanism for reversible hexamer formation. The theoretical percentage of histidine protonation versus pH is calculated using a pKa of 6.07 for the histidine side chain. Monomer percentages of IgG1-RGY are shown as determined by HP-SEC (IgG1-2F8-RGY) and Native MS (IgG1-005-RGY).

theoretical pKa of 6.07. The monomer content of IgG1-RGY at different pH correlated with the fraction of histidine protonation theoretically predicted for fully solvent-accessible side chains (Fig. 1E), which may likely regulate reversible intermolecular Fc-Fc interactions.

Mutation E430G Decreases Conformational Stability at Elevated Temperature in a Reversible Manner

To study the impact of solution hexamerization on antibody behavior and long-term stability we selected antibody IgG1-7D8 (anti-CD20) as a model antibody with regular antibody properties. Previous work showed good stability of the 7D8 antibody[27], and available robust cellular and solution complement activity assays enabled us to monitor potency and aggregation continuously, and to detect heterogeneous biochemical changes. The IgG1-7D8-WT and the IgG1-7D8 variants with introduced mutations showed increased C1q binding and CDC activity on Raji cells in the order WT<E430G/E345K<E345R<RGY (Fig. S3), consistent with previous observations.[9]

Differential Scanning Calorimetry (DSC) was used to study the unfolding of IgG1-7D8-WT, E430G and E345K variants in PBS pH 7.4. In order to eliminate interference by Fab unfolding events, also isolated Fc domains with or without mutations were analyzed. An individual Fc domain containing mutation E430G showed an approximately 8.5°C decrease in the first thermal transition (melting temperature; T_{m1}) compared to a WT Fc-domain. In contrast, an Fc-domain containing Fc-Fc interface mutation E345K showed a T_{m1} similar to WT (Fig. 2A, Table 1). The difference in T_{m1} between E430G and the other variants was less apparent in full length IgG antibodies (Fig. 2B, Table 1), which may be caused by overlapping unfolding events in the Fab-domain and the Fc domain at approximately 60°C (Fig. S4).

The conformational stability of IgG1-7D8 variants WT, E430G, E345K, E345R and RGY in formulations with different pH was assessed by Differential Scanning Fluorimetry (DSF), and the first midpoint of unfolding or melting temperature (T_{m1}) was calculated from the thermal unfolding curves (Fig. 2C, Table 1). WT, E345K and

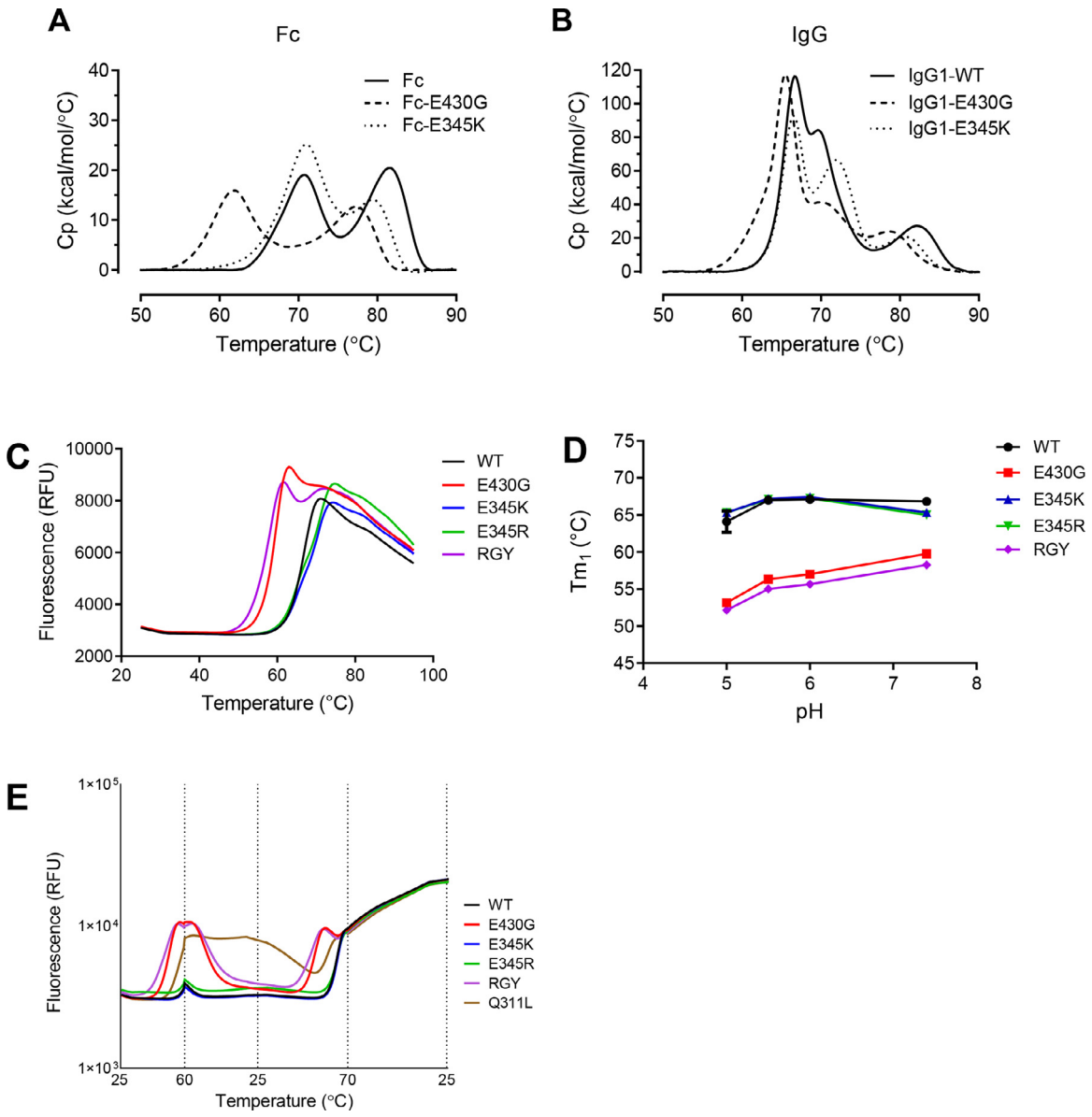

Figure 2. Mutation E430G decreases conformational stability in a reversible manner. (A) Differential Scanning Calorimetry of IgG1-7D8-WT and variants in PBS pH 7.4**.** Comparison between DSC thermograms of WT Fc-domains and Fc domains of variants E430G or E345K. (B) Comparison between DSC thermograms of full length IgG1-7D8-WT and variants E430G or E345K. (C) Differential Scanning Fluorimetry of IgG1-7D8-WT and variants. Unfolding curves in PBS pH 7.4. (D) pH dependence of unfolding by DSF: The first melting temperature (Tm_1), assigned as unfolding of the Fc domain, is plotted versus pH. Average values based on 3 replicate experiments are shown. (E) Reversibility of unfolding in Acetate pH 5.0 as shown by a heating-cooling-heating cycle from 25-60, 60-25, 25-70 and 70-25°C. One representative experiment of two independent repeats is shown.

E345R variants behaved comparably, and the T_{m1} (64-67°C) was not considerably influenced by the pH (Fig. 2D, Table 1). In contrast, variants E430G and RGY, both containing mutation E430G, displayed a decrease in T_{m1} to 58-60°C when analyzed at pH 7.4, consistent with the DSC results. The lower T_{m1} was evident under the different formulation conditions tested, showing a further decrease in T_{m1} value to 52-53°C for E430G and RGY at pH 5.0.

Because E430G was designed to modulate intramolecular Fc domain dynamics, we hypothesized that the decrease in melting temperature could reflect reversible rather than irreversible unfolding. We therefore analyzed the reversibility of the unfolding process at pH 5.0 using a heating-cooling-heating program. Samples were heated from 25 to 60°C, cooled back to 25°C, and subsequently exposed to an additional cycle from 25 to 70°C and reverse (Fig. 2E). Remarkably, the fluorescence signal measured for variant E430G showed an initial increase during heating to 60°C that reverted essentially to baseline level upon cooling down, indicating that variant E430G recovered its original conformation with high efficiency. Reversible unfolding-refolding was also observed upon applying the heating-cooling cycle at pH 6 and 7.4 (data not shown). At all tested pH values, subsequent heating to 70°C caused the antibody to unfold again, but led to an irreversible loss of IgG conformation demonstrated by a sharp increase in fluorescence after cooling down, due to reduced fluorescence quenching of the stably bound dye. WT IgG1 and variants E345K and E345R also irreversibly unfolded after heating to 70°C, but remained largely folded at 60°C. As an example of potential hydrophobicity-driven aggregation, we examined mutation of solvent-exposed amino acid Q311, which potentiated complement activity when mutated to Ile or Leu likely by engaging in hydrophobic Fc-Fc interactions[9], and mutation of which affected both FcRn and protein A binding[28]. In contrast to the other tested mutations, hydrophobic surface mutation Q311L clearly triggered a different pathway,

Table 1
Data overview of biophysical characterization of IgG1-WT and variants. Assays were performed with IgG1-7D8-WT, E430G, E345K, E345R and RGY variants at different pH. Standard deviations based on measurements as indicated in the individual Figures. NM= Not measured. NE= No elution. For DSC measurements, the lower bound of experimental precision was estimated at 0.01°C if the standard error between triplicate measurements was determined at <0.01°C.

Assay	Parameter	pH	WT	E430G	E345K	E345R	RGY
DSC	Tm_1 Fc (°C)	7.4	70.57±0.04	62.04±0.05	70.98±0.03	NM	NM
	Tm_2 Fc (°C)	7.4	81.10±0.03	76.36±0.06	79.38±0.04	NM	NM
	Tm_1 IgG (°C)	7.4	66.34±0.01	65.34±0.04	66.40±0.01	NM	NM
	Tm_2 IgG (°C)	7.4	69.47±0.05	71.50±0.13	71.96±0.02	NM	NM
	Tm_3 IgG (°C)	7.4	81.86±0.04	78.29±0.25	80.56±0.04	NM	NM
DSF	Tm_1 (°C)	7.4	66.8±0.3	59.8±0.3	65.3±0.3	65.0±0.0	58.3±0.3
		6.0	67.1±0.2	57.0±0.0	67.4±0.1	67.3±0.3	55.7±0.3
		5.5	67.0±0.0	56.3±0.3	67.2±0.2	67.1±0.2	55.0±0.0
		5.0	64.1±1.4	53.2±0.3	65.3±0.3	65.3±0.3	52.2±0.3
SIC	B_{22} ($mol \times mL/g^2 \times 10^{-4}$)	7.4	1.3±0.1	0.7±0.1	0.0±0.2	NE	NE
		6.0	1.3±0.1	1.1±0.1	1.3±0.1	-1.1±0.1	NE
		5.0	0.8±0.2	0.9±0.2	1.0±0.1	-0.1±0.2	NE
PEG	$PEG_{midpoint}$ (%PEG)	7.4	16.6±0.3	13.8±0.3	13.0±0.2	10.9±0.2	7.5±0.3

in which the fluorescence signal remained high after heating to 60°C and subsequent cooling down, suggesting irreversible unfolding of this antibody under these conditions. The results indicate that the thermally induced unfolding event observed at 60°C for variants E430G and RGY is a dynamic and reversible process.

The Self-Interaction of Hexamerization-Enhancing IgG Variants can be Controlled by pH and Salt

The self-association of IgG1-7D8 WT, E430G, E345K, E345R and RGY was analyzed by Self-Interaction Chromatography (SIC). This method involves coupling of the antibody to a chromatographic stationary phase and subsequent injection of the same antibody in the mobile phase. The retention on the column is controlled by the (self)-interaction of the antibodies in the two phases. To minimize non-specific binding to the resin, the beads were coupled at antibody concentration of 5 mg/mL and equal coupling densities (8.6-10.5 mg/mL) were confirmed for each variant. The retention time is used to determine the osmotic second virial coefficient (B_{22}) as a measure for self-interaction (specific and non-specific) between two proteins in a dilute protein solution. Negative B_{22} values indicate net attractive protein-protein interactions (increased self-association), whereas positive B_{22} values represent repulsive intermolecular interactions.[29] WT and variant antibodies were coupled to beads that were packed into separate columns and SIC was performed by injecting 1 μL of 1.0 mg/mL of IgG using mobile phases with pH values ranging from 7.4 to 5.0 (Fig. 3, Table 1). WT antibody readily eluted from the column in PBS pH 7.4 containing 140 mM NaCl. When using the histidine (pH 6.0) and acetate buffers (pH 5.0) without salt, none of the tested WT or mutant antibodies eluted off the column. Upon increasing the salt concentration to 80 mM NaCl, WT and single point mutants could be recovered at pH 6.0 and 5.0. In contrast, variant RGY failed to elute under all tested conditions. Variant E345R did not elute in PBS pH 7.4, while histidine or acetate mobile phases stimulated elution. The B_{22} values of E345R were lower than those of WT, suggesting an increased self-interaction for E345R under all conditions tested. Variants E345K and to a lesser extent E430G show a higher tendency for self-association compared to WT at neutral pH, while at lower pH, both variants showed B_{22} values comparable to WT IgG1. Since retention on the column was highly sensitive to even single point mutations introduced into WT IgG1, we interpret their modulation of B_{22} values as modulation of self-interaction. However, a contribution by differences in non-specific binding to the chromatography resin, even at the high IgG-coupling densities applied, could not be excluded.

The Self-Association of Hexamerization-Enhancing IgG Variants Increases In The Order WT<E430G<E345K<E345R<RGY

The behavior of variant RGY suggested that self-association of the other IgG single mutants may also be a dynamic equilibrium process, dependent on antibody concentration and solution conditions. However, HP-SEC and MS are performed at dilute protein concentrations, where weak antibody interactions of the single mutants were not or

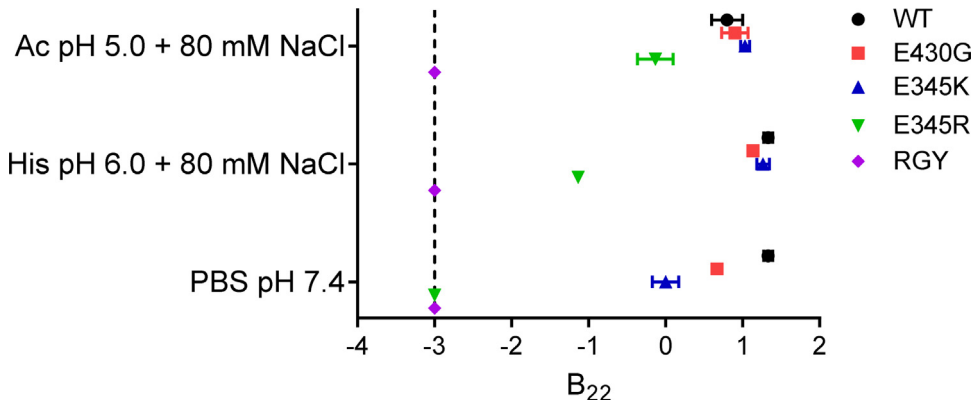

Figure 3. Self-Interaction of hexamerization-enhancing IgG variants can be controlled by pH. Self-Interaction Chromatography of IgG1-7D8-WT and variants in different buffers (PBS pH 7.4, Histidine pH 6.0 + 80 mM NaCl and Acetate pH 5.0 + 80 mM NaCl). Antibodies not eluting from the column are represented as B_{22} value of -3. Error bars represent standard deviation (n= ≥ 3 replicates).

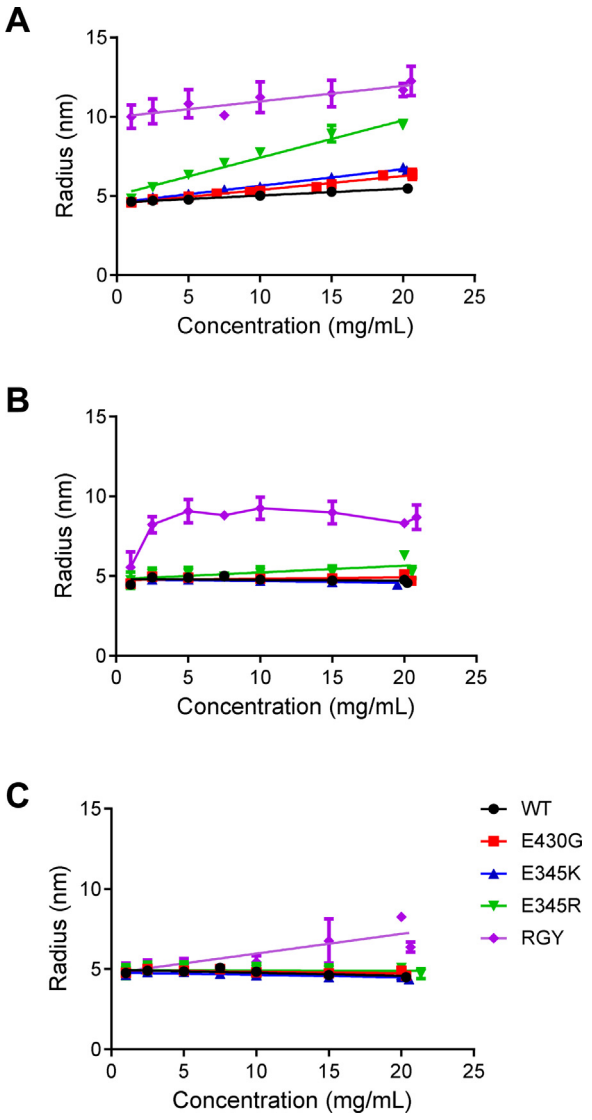

Figure 4. Self-association of hexamerization-enhancing IgG variants increases in the order WT<E430G<E345K<E345R<RGY. Concentration and pH dependence of oligomer formation of IgG1-7D8-WT and variants analyzed by Dynamic Light Scattering. The hydrodynamic radius was determined by DLS at room temperature for the IgG variants at different concentrations in different buffers: (A) PBS pH 7.4. (B) Histidine pH 6.0. (C) Acetate pH 5.0. Error bars represent standard deviation of n = 4 to 6 replicates from n = 2 to 3 independent experiments.

only poorly detectable, due to their transient nature. Since weak Fc-Fc interactions may only become apparent at high concentrations, the self-association of the IgG variants was further analyzed by dynamic light scattering (DLS). DLS is capable of analyzing protein solutions at the concentrations regularly used in therapeutic antibody formulations for intravenous dosing (10-20 mg/mL). Of note, these higher concentrations may simulate antibody interactions at the cell surface after antigen binding, where the antibodies are effectively concentrated due to binding of proximal antigens. The hydrodynamic radius of IgG1-7D8 WT, E430G, E345K, E345R and RGY antibodies was measured by DLS in the concentration range of 1-20 mg/mL (Fig. 4). For all measurements, the size distributions showed one peak (with normal autocorrelation functions), but with different radii and peak width depending on the variant and the concentration (Fig. S5). Likely, the resolving power of DLS was not sufficient to separate monomer and hexamer species, but the presence of increasing hexamer (or intermediate oligomer) content was suggested by peak shifts to a higher radius. An increase in radius with rising concentration is likely caused by increased self-association, but a contribution of potential increasing viscosity cannot be ruled out. Since increased viscosity can be caused by higher protein self-association propensity in concentrated solutions,[30] correcting the radius data for viscosity could underestimate the impact of self-association. In PBS pH 7.4, IgG1-RGY showed an increased radius at all concentrations, indicating formation of oligomers, likely hexamers (Fig. 4A), which have an expected radius of approximately 12-13 nm. The radius of mutant E345R started at monomer level at 1 mg/mL and increased with rising protein concentration, indicating increased self-association compared to WT and other single mutants. Also variant E345K and to a lesser extent E430G showed trends with slightly increased slopes, indicating modestly elevated self-association at neutral pH compared to WT. This self-association at neutral pH increased in the order WT<E430G<E345K<E345R<RGY, consistent with the trend observed in SIC. In the more acidic formulations at pH 5.0 and 6.0, the single mutants behaved like WT IgG at all concentrations (Fig. 4B and C). Interestingly, IgG1-RGY showed a clear biphasic behavior at pH 6.0. While being monomeric at 1 mg/mL, the antibody self-associated at 2.5-5.0 mg/mL, and the radius subsequently remained constant from 5.0-20.0 mg/mL. At pH 5.0, the radius of IgG1-RGY suggested it existed predominantly in monomeric state, while oligomerization was detectable at 15 mg/mL and higher.

PEG-Induced Precipitation Correlates with Colloidal Stability

Polyethylene glycols (PEGs) can be used to assess the solubility of proteins in general,[31, 32] and of monoclonal antibodies specifically.[33, 34] PEGs are water-soluble polymers that can be used to induce protein precipitation, which is assumed to be driven by excluded volume effects.[31] We studied the behavior of IgG1-7D8 antibody variants upon incubation with increasing amounts of PEG, promoting their precipitation. The resulting $PEG_{midpoint}$ values are defined as the PEG percentage (%PEG) at which 50% of the IgG has precipitated. Decreasing $PEG_{midpoint}$ values are indicative of a lower relative solubility profile.[33] When IgG1-7D8-WT, E430G, E345K, E345R and RGY variants were incubated at increasing PEG concentrations in PBS pH 7.4, we observed a trend consistent with the SIC and DLS results, i.e. WT showed the highest relative solubility (highest $PEG_{midpoint}$) followed by E430G/E345K, E345R, and RGY. These data indicate that the PEG assay correlated with colloidal stability assessed by SIC and DLS. When performing the PEG assay at pH 5-6, none of the variants precipitated, even at the highest (22%) PEG concentration (Fig. 5). Thus, decreasing the pH appeared to strongly promote relative antibody solubility.

Real-time Stability of Hexamerization-Enhancing IgG Variants

In general, therapeutic antibody candidates with reduced colloidal and/or conformational stability within an antibody panel are considered less attractive for product development. Hence, we studied the impact of the increased self-association propensity observed for E345K and E430G, and of the decreased conformational stability observed for E430G, on long-term stability. Variants IgG1-7D8 WT, E430G and E345K were chosen for stability assessment as the variants displayed PK profiles similar to wild type IgG1[9], but differed in apparent conformational and colloidal stability. Stability was monitored for 24 months at 2-8°C and for 6 months at 25°C, at the drug formulation-relevant concentration of 20 mg/mL, in PBS pH 7.4 as a non-ideal formulation, and in acetate buffer (30 mM Sodium acetate, 15 mM NaCl, 200 mM D-sorbitol pH 5.0) to minimize self-association. In order to assess aggregate formation during storage, HP-SEC and DLS were performed, both capable of detecting reversible and non-reversible multimers. HP-SEC analysis showed that aggregation of

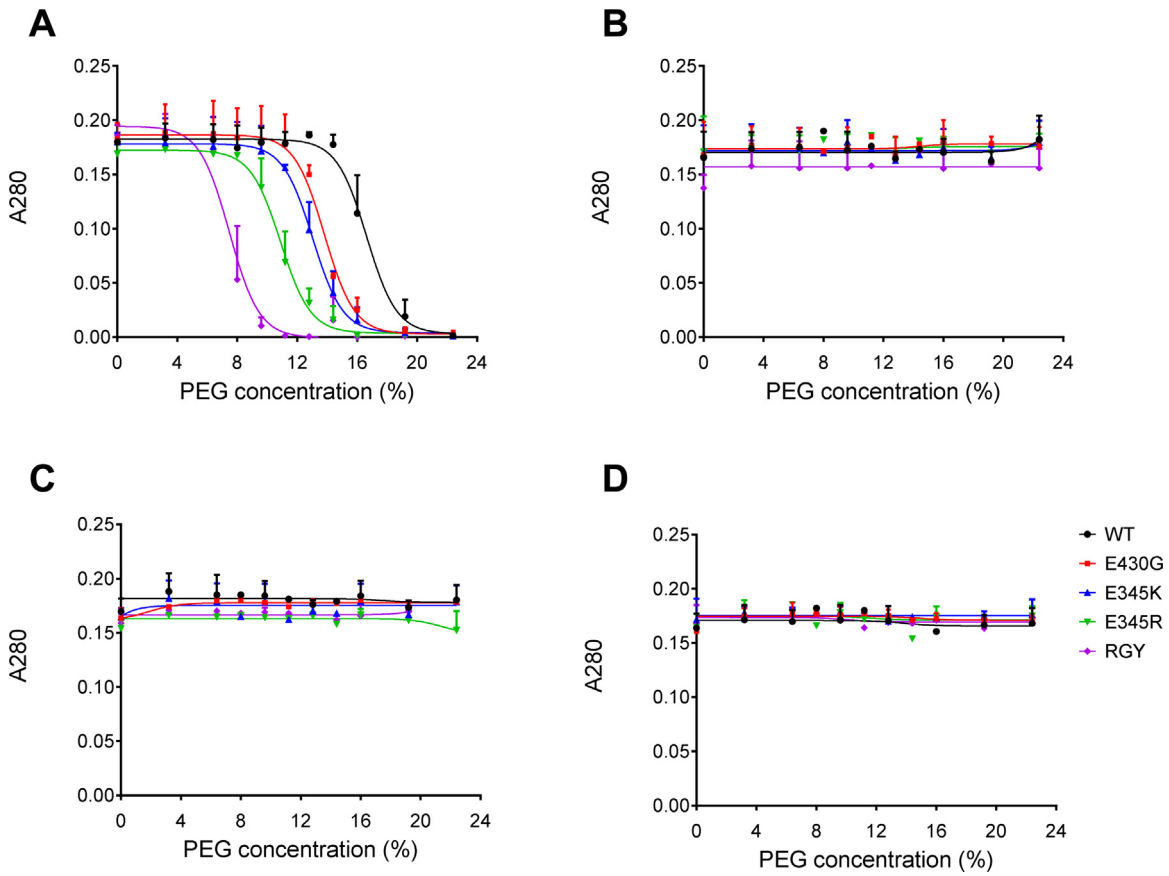

Figure 5. Relative antibody solubility and pH dependence by PEG assay. PEG-induced precipitation of IgG-7D8-WT and variants was determined in different buffers. (A) PBS pH 7.4. (B) Histidine pH 6.0. (C) Acetate pH 5.5. (D) Acetate pH 5.0. Results are based on n = 2 to 4 independent experiments.

WT and both single mutants was minimal at pH 7.4 (<3% multimer formation in 24 months) and absent at pH 5.0 (Fig. 6A). As expected, increased thermal stress at 25°C increased the rate of multimer formation. At both temperatures and in both formulations, variant E430G behaved similar to WT, while variant E345K showed slightly elevated multimer formation.

The average protein radius was monitored over time by DLS (Fig. 6B), which is capable of detecting particles in the size range of ~1 nm to ~10 μm. The somewhat larger size of E430G and E345K at 20 mg/mL at pH 7.4 (respectively 7 and 8 nm radius compared to 6 nm for WT IgG1) likely reflects increased hexamer abundance compared to WT at neutral pH. This increased self-association propensity did not influence the stability of the antibody radius during storage at 2-8°C or 25°C. At pH 5.0, the size of the point mutants was comparable to WT, consistent with complete dissociation of hexamers, and remained stable over time at 2-8°C. Non-reducing CE-SDS showed that the percentage of intact IgG incubated at 2-8°C did not significantly change over time for WT and the mutants, although consistently approximately 5% less intact IgG was observed for E430G (Fig. S6). This apparent increase in antibody fragmentation is contradicted by the absence of fragments in HP-SEC, suggesting that fragmentation of E430G was primarily induced during CE-SDS sample preparation (10 min, 70°C), possibly due to the higher flexibility of E430G. Purity of Heavy + Light Chain by reducing CE-SDS, monomer and degradation level by HP-SEC, polydispersity (Pd) by DLS, antibody concentrations (determined from absorbance measurements at 280 nm by spectrophotometry) and turbidity measurements by absorbance at 350 nm (as a measure for large aggregates) did not show clear differences upon storage for 24 months at 2-8°C (Fig. S6-9). The analysis of sub-visible particles was not included in this research study due to limiting sample volume, but neither DLS, nor A350 measurements indicated the presence of large aggregates during the course of the study.

To supplement the analytical methods focused on specific antibody properties, we assessed the functional stability of the IgG variants by complement activity assays. As expected, both variants E430G and E345K show a 5-7-fold increase in CDC (decrease in EC50) compared to WT at t=0 (Fig. S10). No changes in CDC potency were observed during the course of the study. Additionally, C4d production was monitored over time. The C4d assay measures complement activation in full human serum upon formation of IgG aggregates in solution. Heat-aggregated IgG was used as a positive control. Fluid phase complement activation was stable over time at 2-8°C, and C4d levels in WT, E345K and E430G samples were comparable (Fig 6C). In summary, these data show that the increased self-association of the mutants did not influence their long-term stability at 2-8°C. Moreover, the reduced conformational stability of variant E430G did not affect its long-term stability.

Discussion

In this work, we assessed the colloidal, conformational, and long-term stability of IgG model compounds with stepwise increasing hexamer formation propensity. The chosen IgG model compounds were based on the HexaBody technology for which self-association was driven by the stabilization of interactions at a well-characterized Fc-Fc interface[35, 36] that is also utilized by wild type IgG to promote complement activation.[8, 26] Here, we show that the CDC potency correlated with increased oligomerization propensity at neutral pH demonstrated by different assays,

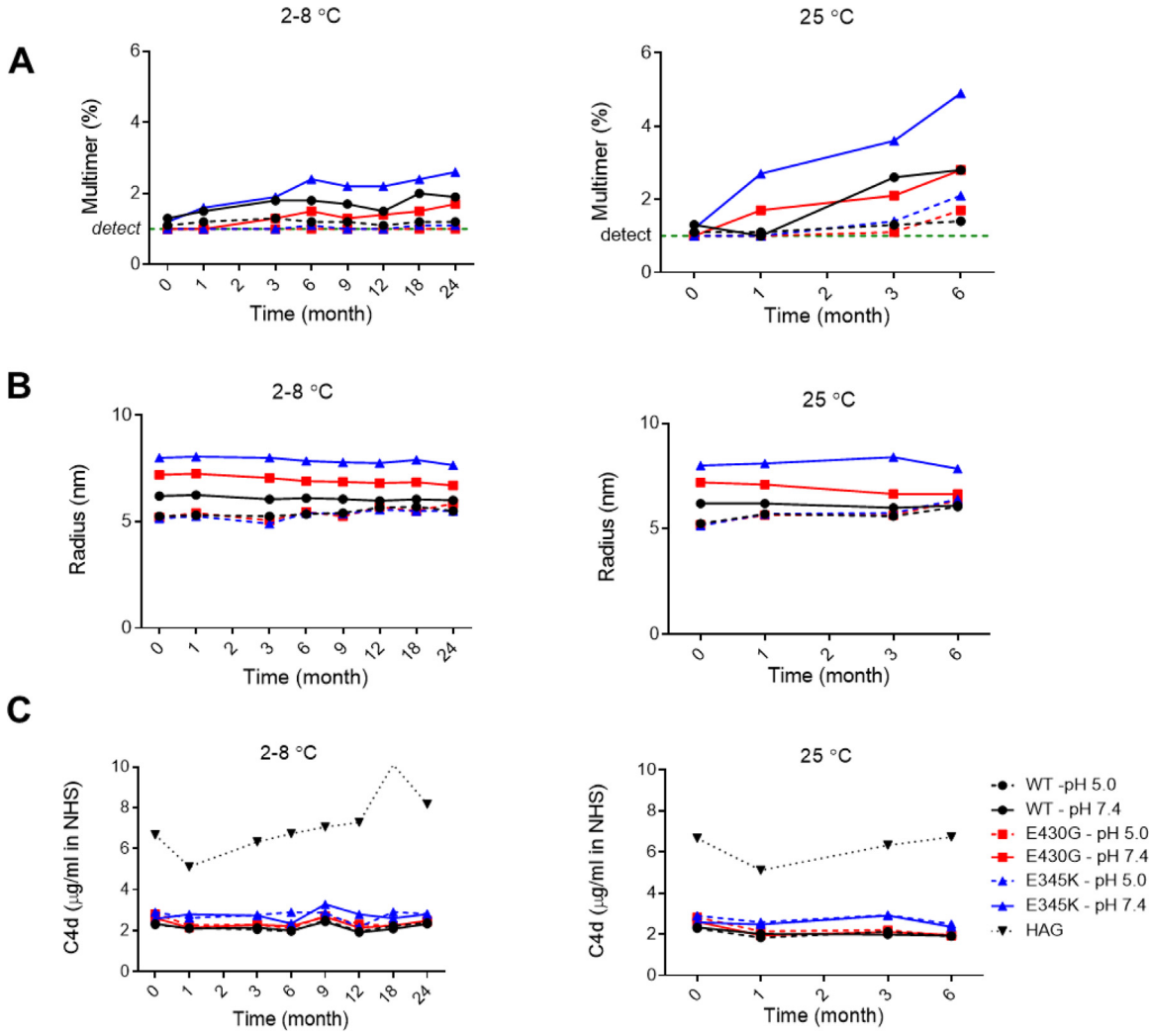

Figure 6. Real-time and accelerated stability of WT, E430G and E345K in two different buffers. Stability of IgG1-7D8-WT, E430G and E345K variants was monitored upon storage at 20 mg/mL during 24 months at 2-8°C (left) and 6 months at 25°C (right) in PBS pH 7.4 (solid line) and Acetate pH 5.0 (dashed line). (A) Multimer formation measured by HP-SEC. (B) Average radius measured by DLS. (C) Target-independent complement activation in C4d assay. Heat-Aggregated IgG (HAG) was used as a positive control.

in the order WT<E430G<E345K<E345R<RGY. The hexamerization process was reversible and strongly dependent on antibody concentration, consistent with equilibrium conditions between monomeric and oligomeric species in solution[24, 37], and with reversible self-association previously described for other antibodies.[18, 19, 22] DLS (performed at a concentration range of 1-20 mg/mL) detected a slight increase in self-association at neutral pH for E345K and to a lesser extent for E430G compared to WT, whereas HP-SEC and native MS failed to do so at the concentrations accessible to these methods. Interestingly, PEG-induced precipitation of the variants in PBS pH 7.4 at low antibody concentrations showed a good qualitative correlation with the DLS measurements and correlated with CDC potency, indicating that PEG-induced precipitation is correlated to IgG hexamerization propensity. Particularly its reduced material requirements may make the PEG assay attractive for the early stage assessment of colloidal stability during developability screening of therapeutic antibody lead panels.

The hexamerization propensity of the antibody model compounds was strongly influenced by pH. Decreasing the pH from 7 to 5 enabled dissociation of IgG1-RGY hexamers in HP-SEC and native MS analyses. Also at the higher antibody concentrations assessed by DLS, single point mutants were completely monomeric in solution at pH 5, while oligomerization of IgG1-RGY was strongly reduced. At pH values of 5 to 6, PEG-induced precipitation of WT and all variants was undetectable. $PEG_{midpoint}$ values also increased upon reduction of the solution pH for other IgG1 antibodies,[33, 34] which correlated well with apparent solubility measured by ultrafiltration.[33] It is unclear to what extent the pH sensitivity of the hexamerization process may impact the activity of HexaBody molecules in tumor microenvironments characterized by acidosis or increased acidity. As a consequence of acidosis, the extracellular pH of solid tumors may decrease to pH 6.5 to 6.9, compared to values of 7.2 to 7.4 for normal tissues.[38] This modest reduction in pH may be expected to reduce hexamerization efficiency and complement activating potency of especially WT IgG molecules, but could be offset by the HexaBody-technology and by the recruitment of C1q, which both may stabilize the hexameric IgG state.

The hexamer dissociation at low pH observed for the RGY variant correlated well with the theoretical protonation state of histidine side chains. Indeed, the Fc-Fc domain interface driving hexamerization contains histidines at positions 310, 433 and 435 also involved in the reversible association with the neonatal Fc receptor FcRn.[39, 40] Of note, putative histidyl protonation had a functional effect opposite to that of removing negative charges in E430 and E345 mutants, suggesting Fc-Fc interactions may be regulated more likely by the local

electrostatic environment than by global charge-charge interactions. Histidyl groups in the CDR regions of Fab fragments may also affect the formulation-dependent self-association of IgG antibodies,[41] proposed to be regulated by salt anion interactions with exposed histidine side chains.[18] Increasing ionic strength can either increase or decrease self-association due to respective shielding of attractive or repulsive electrostatic interactions.

Both colloidal and/or conformational stability may contribute to the rate and extent of aggregation.[42, 43] When we assessed the conformational stability of the IgG variants by DSC and DSF, variants containing mutation E430G showed reduced melting temperatures. In IgG antibodies, C_H3 residue glutamic acid E430 and C_H2 residue lysine K338 form a highly conserved ionic salt bridge. Removal of this salt bridge in mutant E430G promoted IgG hexamerization, which was hypothesized to be dependent on an Fc conformation occupied more frequently after destabilization of the C_H2-C_H3 domain interface,[9] which may be a more "open" conformation as indicated by recent work on N297-hypergalactosylated antibodies.[37] Direct measurement of conformational Fc domain dynamics at physiological temperatures may further improve our understanding.[44] Reversibility of the E430G-promoted unfolding event was shown by DSF using a heating-cooling cycle from 25 to 60°C and back, in which fluorescence signals essentially returned to baseline levels. The observed behavior might be driven by unfolding of the C_H2 domain, which for WT IgG1 was previously observed to be fully reversible up to 65°C.[45] In contrast, an irreversible loss of IgG conformation was observed for all tested antibody variants after heating to 70°C. In contrast to E430G, Fc-Fc interface mutations E345K and E345R did not appreciably affect IgG melting temperatures, indicating that a reduction in conformational stability may promote, but is not required for increased CDC potency. Most likely, E430G and E345K/R promote hexamerization via distinct underlying mechanisms. Because all possible substitutions of E345 promoted CDC, it appears the glutamic acid sidechain is particularly unfavorable to productive Fc-Fc interactions, although the exact mechanism remains poorly understood.[9] The slightly higher hexamerization propensity of E345R compared to E345K may be consistent with a stabilizing interaction with opposing G385 or Q386 as suggested previously.[36]

The developability assessment of antibody panels is steadily gaining interest, and antibodies that display low self-association and high conformational stability are considered to pose fewer downstream risks and thus more optimal for further development.[46] Interestingly, neither the apparent decrease in conformational stability for E430G, nor the increased oligomerization propensity of variants E430G and E345K impacted the stability of these variants compared to WT when monitored for two years at 2-8°C. Our results suggest that the reversibility of processes like self-association and unfolding may affect the eligibility of certain antibody leads for development. We also demonstrated how formulation could impact the biophysical properties of the specific antibody variants studied. Although some variants showed substantial differences compared to WT at neutral pH, their behavior was similar to WT at reduced pH. These observations may argue for the inclusion of different formulations during the developability assessment of antibodies or antibody variants aimed at avidity enhancement via Fc-Fc or Fab-Fab domain interactions after target binding. Further insight into the reversibility of aggregation and unfolding processes under artificially stressed conditions may also improve our ability to predict their impact on the real-time stability and shelf life of therapeutic antibodies.

In summary, the biophysical characterization of the studied antibody variants at elevated concentrations showed that their increasing CDC potency was correlated to their increased self-association propensity in solution. The apparent decrease in conformational stability for E430G, and the increased oligomerization propensity of variants E430G and E345K did not compromise their colloidal stability during long-term storage at 2-8°C.

Materials and Methods

Antibodies, Fc and Fab Subunits

Anti-EGFR mAb IgG1-2F8,[47] anti-CD38 mAb IgG1-005[48] and anti-CD20 mAb 7D8[49] were generated as described before[9]. IgG1-2F8-RGY, IgG1-005-RGY, IgG1-7D8-E345R and IgG1-7D8-RGY antibodies were expressed in ExpiHEK293 FreeStyle cells as described before,[50] and purified by Protein A affinity chromatography. IgG1-7D8-WT, E430G and E345K were expressed from stable CHO-K1 cell lines, purified by protein A affinity chromatograpy and a successive anion exchange purification step.[9] Theoretical pI of the antibodies (calculated with EMBOSS software) ranges from 7.9-8.3.

Fc and Fab subunits of IgG1-7D8-WT, E430G and E345K were generated by digestion of the IgG with papain (Sigma-Aldrich, P4762). Digested material was purified using Protein A affinity chromatography to isolate the Fc fragments. The Fab fragment of IgG1-7D8 was recovered from the flow-through fraction and further purified using gel-filtration.

Buffers

PBS pH 7.4 was purchased (B. Braun, 3623140) and histidine and acetate buffers were prepared from L-histidine (Sigma-Aldrich, 6034), L-histidine-HCl (Sigma-Aldrich, 5659), D-sorbitol (Sigma-Aldrich, 85529), sodium acetate trihydrate (Sigma-Aldrich, 32318) and sodium chloride (Sigma-Aldrich, 31434). The following buffers with corresponding abbreviations were used throughout the study unless stated otherwise: PBS pH 7.4: 10.6 mM Sodium phosphate, 140 mM NaCl, pH 7.4. Histidine pH 6.0: 30 mM Histidine, 225 mM D-sorbitol pH 6.0. Acetate pH 5.5: 30 mM Sodium acetate, 15 mM NaCl, 200 mM D-sorbitol pH 5.5. Acetate pH 5.0: 30 mM Sodium acetate, 15 mM NaCl, 200 mM D-sorbitol pH 5.0.

Capillary Electrophoresis – Sodium Dodecyl Sulfate (CE-SDS)

Purity and fragmentation of the samples was analyzed using CE-SDS on the Labchip GXII (Caliper Life Sciences). Sample preparation was performed with the HT Protein Express Reagent Kit (Perkin Elmer, 760328) according to manufacturer's instructions (High Sensitivity protocol) with few modifications. The denaturing step was performed using 5 μL sample (at 1 mg/mL) + 7 μL denaturing solution + 32 μL Milli-Q water and incubation at 70°C for 10 min. Analysis was performed under both non-reducing and reducing conditions (addition of 1,4-dithiothreitol). Protein size (kDa) and purity (%) were analyzed using the Labchip GX Reviewer software.

CDC Assay

CDC assays were performed as described[51] with normal human serum (20% final concentration) as a source of complement. The Raji cell line (human lymphoma) was obtained from the American Type Culture Collection (ATCC no. CCL-86). Fraction lysis was determined as the fraction propidium iodide (PI) (+) cells of total cells (%) using an iQue flow cytometer (Intellicyt®, Sartorius).

Complement Activation in Normal Human Serum

Complement activation in the absence of target was determined by measuring C4d concentrations, after incubating 100 μg antibody per mL in 90% normal human serum for 1 h at 37°C. C4d

concentrations were measured in an ELISA (MicroVue C4d EIA kit, Quidel Corporation) according to manufacturer's instructions.

Differential Scanning Calorimetry (DSC)

DSC was performed using a MicroCal VP-Capillary DSC system. Samples were analyzed at 0.5 mg/ml in PBS pH 7.4. Thermograms were acquired between 10 and 100°C at 60°C/h scanning rate. The calorimetric enthalpy was determined by integrating the area under the peak after adjusting the pre- and post-transition baseline. The Van 't Hoff enthalpy of unfolding was determined by fitting thermograms to a non-2-state reversible unfolding model using non-linear least squares fitting.

Differential Scanning Fluorimetry (DSF)

The midpoint of unfolding (melting temperature, T_m)[52] was determined by DSF. Sypro Orange dye (Sigma-Aldrich, S5692) was diluted 320-fold in PBS, Histidine pH 6.0, Acetate pH 5.5 and Acetate pH 5.0. A volume of 5 μL antibody sample (at 1 mg/mL in the corresponding buffer) was added to 20 μL diluted Sypro Orange in iCycler iQ 96-well PCR plates. Fluorescence was measured on a Bio-Rad iQ5 Multicolor Real-Time PCR detection system at increasing temperature from 25°C to 95°C in increments of 0.5°C (Excitation 485 nm, Emission 575 nm) or at other temperature cycles as indicated. Data was analyzed using Bio-Rad CFX Manager Software 3.0 and melting temperatures were determined from the fluorescence versus temperature graphs by the software.

Dynamic Light Scattering (DLS)

Antibody concentration series (1-20 mg/mL) were prepared in different buffers: PBS pH 7.4, Histidine pH 6.0 and Acetate 5.0. DLS measurements were performed on a DynaPro Plate Reader II (Wyatt Technology) with Dynamics 7 software. Samples were applied in duplicate in a 384-well plate (Aurora Biotechnologies, 1011–00110) at 20 μL volume, covered with paraffin oil and the plates were centrifuged for 3 min at 2,111 xg. Ten acquisitions of 5 sec at 25°C were recorded. The cumulant fit was used to analyze the data, using a cut-off value of 2.1 nm, excluding peaks with lower radius, as often caused by software artifacts. A refractive index of 1.333 and a viscosity of 1.019 cP was used. No data correction was made for possible deviations in viscosity due to the formulation.

Thermal scan measurements for determination of T_{agg} were performed using increasing temperature (1°C increase/data point). Data was processed in Excel to determine T_{agg} by calculating the mean and standard deviation (first 10 measurements) of the radius. By setting a 99.99%-confidence interval for each measurement, the first sequential value outside the confidence interval was tagged as T_{agg}.

High Performance Size-Exclusion Chromatography (HP-SEC)

HP-SEC was performed using a Waters Alliance 2975 separation unit (Waters), a TSK G3000SWxl column (Tosoh Biosciences, 0008541) and a TSK-gel SWxl guard column (Tosoh Biosciences, 0008543), using 50 μL injections and flow rate of 1 mL/min. For testing concentration dependence, a concentration series of IgG1-2F8-RGY (0.11-2.5 mg/mL in PBS pH 7.4) was analyzed with PBS pH 7.4 as mobile phase. For testing pH dependence, buffers at pH 5.0, 5.5, 6.0, 6.5 and 7.0 were prepared by mixing 100 mM sodium phosphate (Sigma-Aldrich, 71633) and 50 mM citric acid (Sigma-Aldrich, C1909)/150 mM NaCl (Sigma-Aldrich, 31434). IgG1-2F8-RGY was buffer exchanged to each buffer with Amicon Ultra 10K centrifugal filters (UFC501096). Injections at 2.5 mg/mL antibody were analyzed with the corresponding buffer as mobile phase. For long-term stability, samples were analyzed at 5 mg/mL with 0.1 M sodium phosphate (Sigma-Aldrich 17844/71633), 0.1 M sodium sulfate (Sigma-Aldrich, 31481), pH 6.8 as mobile phase.

Real-Time Stability

Real-time and accelerated stability of IgG1-7D8-E430G, IgG1-7D8-E345K and IgG1-7D8-WT as reference was examined at 20 mg/mL in PBS pH 7.4 and Acetate pH 5.0 buffer. Aliquots of 300 μL were incubated at 2-8°C for 24 months and at 25°C for 6 months. Samples at t=1, 3, 6, 9, 12, 18 and 24 months were analyzed by HP-SEC, CE-SDS, DLS, spectrophotometry, CDC and C4d assay.

Relative Solubility by PEG-Induced Precipitation

PEG-induced precipitation was performed in PBS pH 7.4, Histidine pH 6.0, Acetate pH 5.5 and Acetate pH 5.0. In a UV Star half area plate (Greiner Bio-one, 675801), 20 μL antibody (at 0.8-1.2 mg/mL) was added to 80 μL buffer of varying PEG concentrations from 0-28% (w/v) PEG. The plate was shaken for 5 min at 750 rpm and incubated over night at room temperature. The plates were centrifuged to remove precipitated antibody (12 min, 4000 rpm) and 80 μL was transferred to a new plate. Absorbance at 280 nm (A280) was measured on a Synergy HT Microplate reader. The A280 values were plotted versus the PEG concentration in Graphpad Prism 8 and analyzed using non-linear regression by fitting to the $PEG_{midpoint}$ model described previously[33], in which the $PEG_{midpoint}$ (%) reflects the PEG concentration at which 50% of the antibody was precipitated.

Self-Interaction Chromatography

SIC experiments were performed by Soluble Therapeutics, Birmingham, Alabama. A guard column was packed with Biogel P-6DG dry beads (Biorad) and flow packed using HPLC with PBS pH 7.4 as mobile phase. For preparation of SIC column material, Toyopearls AF-Tresyl 650 (Tosoh Bioscience) were incubated with 2 μL of antibody solution (5 mg/mL in PBS) and subsequently exposed to 0.5 M ethanolamine to cap the unreacted thiol groups on the beads.

Each antibody variant was coupled to beads that were packed into separate columns. Chromatography was performed by a 1 μL injection of a solution containing 1 mg/mL of the identical antibody and 1% (v/v) of acetone in PBS. Different buffers were used as the mobile phase with a flow rate of 8 μL/min: PBS pH 7.4, Histidine pH 6.0, Acetate pH 5.5 and Acetate pH 5.0. NaCl (to a concentration of 80 mM) was added to buffers to enhance protein elution. B_{22} values were calculated based on protein retention times as described before.[53]

Spectrophotometry

Absorbance measurements at 280 nm (A280) were performed in 96-well plates (UV star, Greiner Bio-one, 675801) on a Synergy HT Microplate reader, using 20-fold diluted samples. Antibody concentrations were calculated from Beer's law using the theoretical extinction coefficient for the specific molecule (determined by mEMBOSS software) and the measured A280, after correction for dilution and path length. Absorbance at 350 nm (A350) was determined of the undiluted sample using a NanoDrop ND-1000 spectrophotometer (Isogen Life Science).

Additional methods Cell Culture and Reagents, C1q binding assay, Native MS and Visualization of Antibody Structure are available online, deposited as Supplementary Information.

Declaration of Competing Interests

Yes.

Acknowledgements

The authors wish to thank Klara Beslmüller, Ramon van den Boogaard, Marleen Voorhorst, Jeroen Brouwer, Soeniel Jhakrie, Demelza Willemsz, Mina Chenani, Chantal de Bije, Marlies Gouw, Martijn Kort, Niels Kaldenhoven, Marcel Roza and Rik Rademaker for technical support and valuable scientific contributions. The authors wish to thank Chrysanty Weaver and John McCarter from Soluble Therapeutics (now Soluble Bioscience) for performing SIC analysis and valuable discussions. GW and AJRH acknowledge support from the Netherlands Organization for Scientific Research (NWO) funding the Netherlands Proteomics Centre through the X-omics Road Map program (project 184.034.019), and the NWO Satin Grant 731.017.202.

Data Availability Statement

All data analyzed during this study are included in this published article (and its supplementary information files).

Disclosure of Interest

EvdB, FJB, JS, LKdW, MDvK, MvE, PRB, PWHIP, and RNdJ hold Genmab stocks and/or warrants. EvdB, FJB, JS, MDvK, PWHIP, and RNdJ are inventors on Genmab patent applications. In this manuscript we described the characterization of IgG variants based on, or derived from, the therapeutic antibody platform registered under the trade name “HexaBody.”

Supplementary Materials

Supplementary material associated with this article can be found in the online version at doi:10.1016/j.xphs.2022.02.016.

References

1. Chiu ML, Goulet DR, Teplyakov A, Gilliland GL. Antibody structure and function: the basis for engineering therapeutics. *Antibodies (Basel)*. 2019;8.
2. Wang X, Mathieu M, Brezski RJ. IgG Fc engineering to modulate antibody effector functions. *Protein Cell*. 2018;9:63–73.
3. Labrijn AF, Janmaat ML, Reichert JM, Parren P. Bispecific antibodies: a mechanistic review of the pipeline. *Nat Rev Drug Discov*. 2019;18:585–608.
4. Goldberg BS, Ackerman ME. Antibody-mediated complement activation in pathology and protection. *Immunol Cell Biol*. 2020;98:305–317.
5. J.T. Patel KPR, Barb AW. Multiple variables at the leukocyte cell surface impact Fc gamma receptor-dependent mechanisms. *Front Immunol*. 2019;10:223.
6. Rosenberg AS. Effects of protein aggregates: an immunologic perspective. *AAPS J*. 2006;8:E501–E507.
7. Melis JP, Strumane K, Ruuls SR, Beurskens FJ, Schuurman J, Parren PW. Complement in therapy and disease: regulating the complement system with antibody-based therapeutics. *Mol Immunol*. 2015;67:117–130.
8. Diebolder CA, Beurskens FJ, de Jong RN, Koning RI, Strumane K, Lindorfer MA, et al. Complement is activated by IgG hexamers assembled at the cell surface. *Science*. 2014;343:1260–1263.
9. de Jong RN, Beurskens FJ, Verploegen S, Strumane K, van Kampen MD, Voorhorst M, et al. A novel platform for the potentiation of therapeutic antibodies based on antigen-dependent formation of IgG hexamers at the cell surface. *PLoS Biol*. 2016;14: e1002344.
10. Overdijk MB, Strumane K, Beurskens FJ, Ortiz Buijsse A, Vermot-Desroches C, Vuillermoz BS, et al. Dual epitope targeting and enhanced hexamerization by DR5 antibodies as a novel approach to induce potent antitumor activity through DR5 agonism. *Mol Cancer Ther*. 2020;19:2126–2138.
11. Zhang D, Goldberg MV, Chiu ML. Fc Engineering approaches to enhance the agonism and effector functions of an anti-OX40 antibody. *J Biol Chem*. 2016;291:27134–27146.
12. Roberts CJ. Therapeutic protein aggregation: mechanisms, design, and control. *Trends Biotechnol*. 2014;32:372–380.
13. Kalonia C, Toprani V, Toth R, Wahome N, Gabel I, Middaugh CR, et al. Effects of protein conformation, apparent solubility, and protein-protein interactions on the rates and mechanisms of aggregation for an igg1monoclonal antibody. *J Phys Chem B*. 2016;120:7062–7075.
14. Roberts CJ. Protein aggregation and its impact on product quality. *Curr Opin Biotechnol*. 2014;30:211–217.
15. Moussa EM, Panchal JP, Moorthy BS, Blum JS, Joubert MK, Narhi LO, et al. Immunogenicity of therapeutic protein aggregates. *J Pharm Sci*. 2016;105:417–430.
16. Ratanji KD, Derrick JP, Dearman RJ, Kimber I. Immunogenicity of therapeutic proteins: influence of aggregation. *J Immunotoxicol*. 2014;11:99–109.
17. Rojko JL, Evans MG, Price SA, Han B, Waine G, DeWitte M, et al. Formation, clearance, deposition, pathogenicity, and identification of biopharmaceutical-related immune complexes: review and case studies. *Toxicol Pathol*. 2014;42:725–764.
18. Esfandiary R, Parupudi A, Casas-Finet J, Gadre D, Sathish H. Mechanism of reversible self-association of a monoclonal antibody: role of electrostatic and hydrophobic interactions. *J Pharm Sci*. 2015;104:577–586.
19. Kanai S, Liu J, Patapoff TW, Shire SJ. Reversible self-association of a concentrated monoclonal antibody solution mediated by Fab-Fab interaction that impacts solution viscosity. *J Pharm Sci*. 2008;97:4219–4227.
20. Wu SJ, Luo J, O'Neil KT, Kang J, Lacy ER, Canziani G, et al. Structure-based engineering of a monoclonal antibody for improved solubility. *Protein Eng Des Sel*. 2010;23:643–651.
21. Schrag JD, Picard ME, Gaudreault F, Gagnon LP, Baardsnes J, Manenda MS, et al. Binding symmetry and surface flexibility mediate antibody self-association. *MAbs*. 2019;11:1300–1318.
22. Gentiluomo L, Roessner D, Streicher W, Mahapatra S, Harris P, Friess W. Characterization of native reversible self-association of a monoclonal antibody mediated by FAB-FAB interaction. *J Pharm Sci*. 2020;109:443–451.
23. Nishi H, Miyajima M, Wakiyama N, Kubota K, Hasegawa J, Uchiyama S, et al. Fc domain mediated self-association of an IgG1 monoclonal antibody under a low ionic strength condition. *J Biosci Bioeng*. 2011;112:326–332.
24. Wang G, de Jong RN, van den Bremer ET, Beurskens FJ, Labrijn AF, Ugurlar D, et al. Molecular basis of assembly and activation of complement component C1 in complex with immunoglobulin G1 and antigen. *Mol Cell*. 2016;63:135–145.
25. Ugurlar D, Howes SC, de Kreuk BJ, Koning RI, de Jong RN, Beurskens FJ, et al. Structures of C1-IgG1 provide insights into how danger pattern recognition activates complement. *Science*. 2018;359:794–797.
26. Strasser J, de Jong RN, Beurskens FJ, Wang G, Heck AJR, Schuurman J, et al. Unraveling the macromolecular pathways of IGG oligomerization and complement activation on antigenic surfaces. *Nano Lett*. 2019;19:4787–4796.
27. Gramer MJ, van den Bremer ET, van Kampen MD, Kundu A, Kopfmann P, Etter E, et al. Production of stable bispecific IgG1 by controlled Fab-arm exchange: scalability from bench to large-scale manufacturing by application of standard approaches. *MAbs*. 2013;5:962–973.
28. Zwolak A, Leettola CN, Tam SH, Goulet DR, Derebe MG, Pardinas JR, et al. Rapid purification of human bispecific antibodies via selective modulation of protein A binding. *Sci Rep*. 2017;7:15521.
29. Quigley A, Williams DR. The second virial coefficient as a predictor of protein aggregation propensity: a self-interaction chromatography study. *Eur J Pharm Biopharm*. 2015;96:282–290.
30. Liu J, Nguyen MD, Andya JD, Shire SJ. Reversible self-association increases the viscosity of a concentrated monoclonal antibody in aqueous solution. *J Pharm Sci*. 2005;94:1928–1940.
31. Atha DH, Ingham KC. Mechanism of precipitation of proteins by polyethylene glycols. Analysis in terms of excluded volume. *J Biol Chem*. 1981;256:12108–12117.
32. Arakawa T, Timasheff SN. Mechanism of poly(ethylene glycol) interaction with proteins. *Biochemistry*. 1985;24:6756–6762.
33. Gibson TJ, McCarty K, McFadyen IJ, Cash E, Dalmonte P, Hinds KD, et al. Application of a high-throughput screening procedure with PEG-induced precipitation to compare relative protein solubility during formulation development with IgG1 monoclonal antibodies. *J Pharm Sci*. 2011;100:1009–1021.
34. Toprani VM, Joshi SB, Kueltzo LA, Schwartz RM, Middaugh CR, Volkin DB. A micro-polyethylene glycol precipitation assay as a relative solubility screening tool for monoclonal antibody design and formulation development. *J Pharm Sci*. 2016;105:2319–2327.
35. Saphire EO, Parren PW, Pantophlet R, Zwick MB, Morris GM, Rudd PM, et al. Crystal structure of a neutralizing human IGG against HIV-1: a template for vaccine design. *Science*. 2001;293:1155–1159.
36. Davies AM, Jefferis R, Sutton BJ. Crystal structure of deglycosylated human IgG4-Fc. *Mol Immunol*. 2014;62:46–53.
37. van Osch TLJ, Nouta J, Derksen NIL, van Mierlo G, van der Schoot CE, Wuhrer M, et al. Fc Galactosylation promotes hexamerization of human IgG1, leading to enhanced classical complement activation. *J Immunol*. 2021;207:1545–1554.
38. Ibrahim-Hashim A, Estrella V. Acidosis and cancer: from mechanism to neutralization. *Cancer Metastasis Rev*. 2019;38:149–155.
39. Raghavan M, Bonagura VR, Morrison SL, Bjorkman PJ. Analysis of the pH dependence of the neonatal Fc receptor/immunoglobulin G interaction using antibody and receptor variants. *Biochemistry*. 1995;34:14649–14657.
40. Shields RL, Namenuk AK, Hong K, Meng YG, Rae J, Briggs J, et al. High resolution mapping of the binding site on human IgG1 for Fc gamma RI, Fc gamma RII, Fc gamma RIII, and FcRn and design of IgG1 variants with improved binding to the Fc gamma R. *J Biol Chem*. 2001;276:6591–6604.
41. Yadav S, Laue TM, Kalonia DS, Singh SN, Shire SJ. The influence of charge distribution on self-association and viscosity behavior of monoclonal antibody solutions. *Mol Pharm*. 2012;9:791–802.
42. Goldberg DS, Bishop SM, Shah AU, Sathish HA. Formulation development of therapeutic monoclonal antibodies using high-throughput fluorescence and static light scattering techniques: role of conformational and colloidal stability. *J Pharm Sci*. 2011;100:1306–1315.
43. He F, Woods CE, Becker GW, Narhi LO, Razinkov VI. High-throughput assessment of thermal and colloidal stability parameters for monoclonal antibody formulations. *J Pharm Sci*. 2011;100:5126–5141.

44. Wei B, Gao X, Cadang L, Izadi S, Liu P, Zhang HM, et al. Fc galactosylation follows consecutive reaction kinetics and enhances immunoglobulin G hexamerization for complement activation. *MAbs*. 2021;13:1893427.
45. Zhang-van Enk J, Mason BD, Yu L, Zhang L, Hamouda W, Huang G, et al. Perturbation of thermal unfolding and aggregation of human IgG1 Fc fragment by Hofmeister anions. *Mol Pharm*. 2013;10:619–630.
46. Jain T, Sun T, Durand S, Hall A, Houston NR, Nett JH, et al. Biophysical properties of the clinical-stage antibody landscape. *Proc Natl Acad Sci U S A*. 2017;114:944–949.
47. Bleeker WK, Lammerts van Bueren JJ, van Ojik HH, Gerritsen AF, Pluyter M, Houtkamp M, et al. Dual mode of action of a human anti-epidermal growth factor receptor monoclonal antibody for cancer therapy. *J Immunol*. 2004;173:4699–4707.
48. de Weers M, Tai YT, van der Veer MS, Bakker JM, Vink T, Jacobs DC, et al. Daratumumab, a novel therapeutic human CD38 monoclonal antibody, induces killing of multiple myeloma and other hematological tumors. *J Immunol*. 2011;186:1840–1848.
49. Teeling JL, French RR, Cragg MS, van den Brakel J, Pluyter M, Huang H, et al. Characterization of new human CD20 monoclonal antibodies with potent cytolytic activity against non-Hodgkin lymphomas. *Blood*. 2004;104:1793–1800.
50. Vink T, Oudshoorn-Dickmann M, Roza M, Reitsma JJ, de Jong RN. A simple, robust and highly efficient transient expression system for producing antibodies. *Methods*. 2014;65:5–10.
51. Pawluczkowycz AW, Beurskens FJ, Beum PV, Lindorfer MA, van de Winkel JG, Parren PW, et al. Binding of submaximal C1q promotes complement-dependent cytotoxicity (CDC) of B cells opsonized with anti-CD20 mAbs ofatumumab (OFA) or rituximab (RTX): considerably higher levels of CDC are induced by OFA than by RTX. *J Immunol*. 2009;183:749–758.
52. Ericsson UB, Hallberg BM, Detitta GT, Dekker N, Nordlund P. Thermofluor-based high-throughput stability optimization of proteins for structural studies. *Anal Biochem*. 2006;357:289–298.
53. Johnson DH, Wilson WW, DeLucas LJ. Protein solubilization: a novel approach. *J Chromatogr B*. 2014;971:99–106.